Thermal Structure Along 4°W in the Gulf of Guinea During 1983–1984

ROBERT W. HOUGHTON

Lamont-Doherty Geological Observatory of Columbia University, Palisades, New York

CHRISTIAN COLIN

Office de la Recherche Scientifique et Technique Outre-Mer, Department of Marine, Earth and Atmospheric Sciences
North Carolina State University, Raleigh

SEQUAL/FOCAL data from 4°W derived from conductivity, temperature, and depth, expendable bathythermograph, and aircraft-deployed expendable bathythermograph sections and moored thermistor time series are combined to investigate the thermal structure in the Gulf of Guinea for 1983 and 1984. The equatorial and coastal upwellings, as defined by vertical isotherm displacements, have the same magnitude for both years. The seasonal upwelling extends to at least 300 m depth with the signal at depth leading the surface. The equatorial upwelling occurs approximately 6 weeks earlier in 1983 than in 1984, while the coastal upwelling is only 2 weeks earlier in 1983. The meridional structure of the upwelling is approximately symmetric about the equator at depth but becomes asymmetric, shifted to the south, near the surface. During early 1984 the thermocline is anomalously deep, nearly 30 m below the climatic mean. Because of distinct interannual differences in the wind field it is possible to identify the influence of local and far-field wind forcing on the thermal structure. The main annual "summer" equatorial upwelling is forced primarily by the zonal wind stress distributed westward across the ocean basin. The increasing asymmetry about the equator in the eastern Gulf of Guinea suggests the influence of the local meridional wind stress. The coastal upwelling is coupled to the Guinea Current. The anomalously deep thermocline that persisted in early 1984 is the result of both local and far-field changes in the zonal wind stress.

1. INTRODUCTION

The large sea surface temperature (SST) fluctuations observed in the Gulf of Guinea [*Merle*, 1980; *Hastenrath and Lamb*, 1977] result from the influence of ocean dynamics on a shoaling thermocline in the eastern basin of the equatorial Atlantic Ocean. In particular, there is the annual equatorial upwelling during June and July forced by the intensification of the trade winds, which in combination with the westward South Equatorial Current (SEC) produces a tongue of cold water extending westward from the eastern boundary to approximately 20°W. At approximately the same time there is a coastal upwelling along the northern boundary of the Gulf of Guinea producing a band of cold water from 1°E to 7°W. Considerably weaker upwelling events also occur in December–January.

This study was motivated by previous investigations of these two upwelling regions by *Bakun* [1978], *Berrit* [1976], *Hisard and Merle* [1979], *Houghton* [1976, 1983], *Ingham* [1970], *Longhurst* [1964], *Verstraete* [1970], and *Voituriez* [1981]. There had been difficulty in correlating the Gulf of Guinea upwelling events with local wind forcing. This led to the suggestion of remote forcing [*Moore et al.*, 1978; *Adamec and O'Brien*, 1978; *McCreary et al.*, 1983; *Picaut*, 1983; *Servain et al.*, 1982] whereby winds in the west generate equatorially trapped Kelvin waves that propagate eastward into the Gulf of Guinea and then poleward along the eastern boundary. However, much of the analysis to support this hypothesis is based on historical data with poor spatial and temporal resolution or with SST, which does not always correlate with the underlying thermal structure.

For this reason the combined field program of the Seasonal Response of the Equatorial Atlantic (SEQUAL) experiment and the Français Océan et Climat dans l'Atlantique Équatorial (FOCAL) program in the Gulf of Guinea was designed to observe the thermal structure over a 2-year period with a frequency sufficient to resolve the major upwelling events at the equator and the coast. The objective was to establish whether there is a connection between these regions and to distinguish between local and far-field wind forcing. As a component of the SEQUAL/FOCAL program, the objective was to place the Gulf of Guinea upwelling in the larger context of the ocean response throughout the equatorial Atlantic to the basin-wide wind forcing.

This paper will present a description of the thermal data acquired along 4°W between the coast and the equator in the Gulf of Guinea. The field program and data sources are described in section 2. A description of the thermal field with analysis is given in section 3, and discussion follows in sections 4 and 5.

2. DATA

The combined SEQUAL/FOCAL field program is shown in Figure 1. From July 1982 through October 1984 along 4°W there were nine FOCAL hydrographic sections [*Henin et al.*, 1986] and 18 SEQUAL aircraft-deployed expendable bathythermograph (AXBT) sections [*Mele and Houghton*, 1985]. Additional expendable bathythermograph (XBT) sections are obtained from SEQUAL cruises [*Mele and Katz*, 1985] and the ship of opportunity XBT line (J. Bruce, personal communication, 1985) that crosses 4°W at 9°S. On the equator during much of this period there was a mooring with thermistors at 1, 10, 35, 60, 85, 110, and 310 m depths [*Colin et al.*, 1986]. At the shelf break at 5°N there was a mooring with thermistors at 8, 18, 30, 45, and 60 m depths. Additional thermal data are obtained from weekly GOSSTCOMP SST maps (from National Oceanic and Atmospheric Administration/National Environmental Satellite Service, Satellite
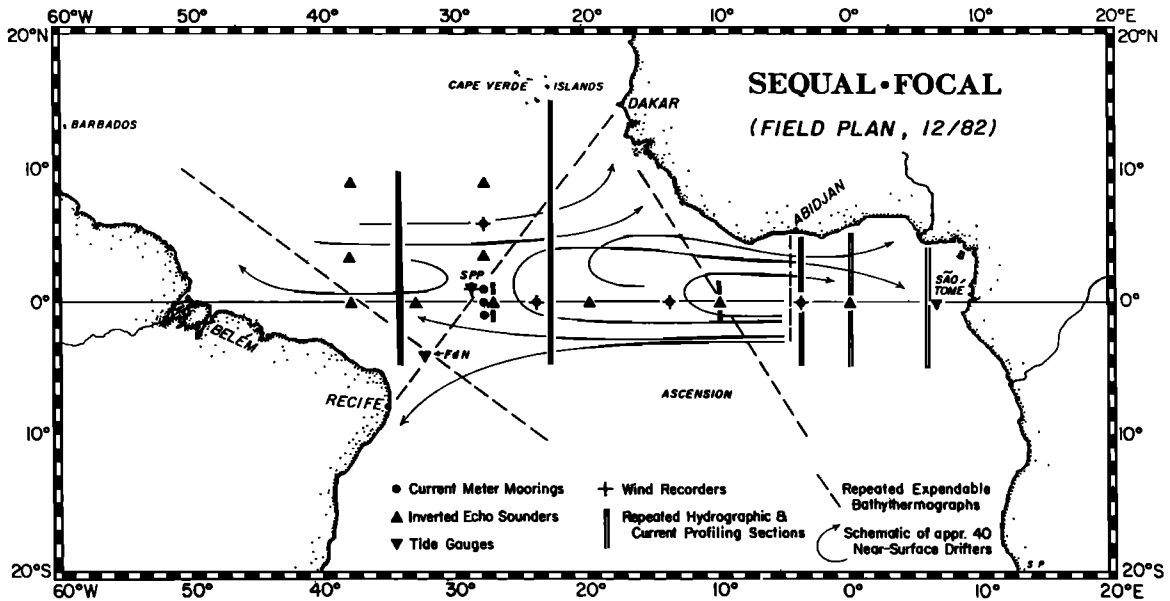
Fig. 1.   SEQUAL/FOCAL field program showing the relation of the Gulf of Guinea AXBT and hydrographic sections to other field work in the equatorial basin.

Data Services Division, Washington, D. C.) covering the entire Gulf of Guinea.

The wind field was measured by near-surface recorders on the St. Peter and St. Paul rocks at 1°N, 29°W [*Garzoli and Katz*, 1984], at the coast near Abidjan (5°N, 4°W), and at the equatorial moorings at 24°W, 14°W, and 4°W. However, only data from 29°W and 4°W (Figure 3) are relatively complete and are analyzed in more detail by C. Colin and S. L. Garzoli (unpublished manuscript, 1986).

The distribution of the sections along 4°W is shown in a time-latitude plot in Figure 2. The FOCAL sections extend to 5°S and consist of conductivity, temperature, and depth (CTD) and current profiles to 500 m depth taken every 1/2° latitude.

These sections, repeated approximately every 3 months, provide the basic information on the seasonal hydrographic structure in the Gulf of Guinea but are not frequent enough to resolve the more rapid upwelling events. This resolution is achieved when the CTD and AXBT sections are combined. Each AXBT section consists of approximately 24 profiles to 350 m depth (300 m at the coast and equator), spaced every 1/2° latitude on the southbound flight from Abidjan, with the remainder distributed on the northbound flight. Although the intention was to schedule these flights (every 10 days) during the onset of the upwelling, the availability of the aircraft resulted in an uneven distribution, especially in 1983.
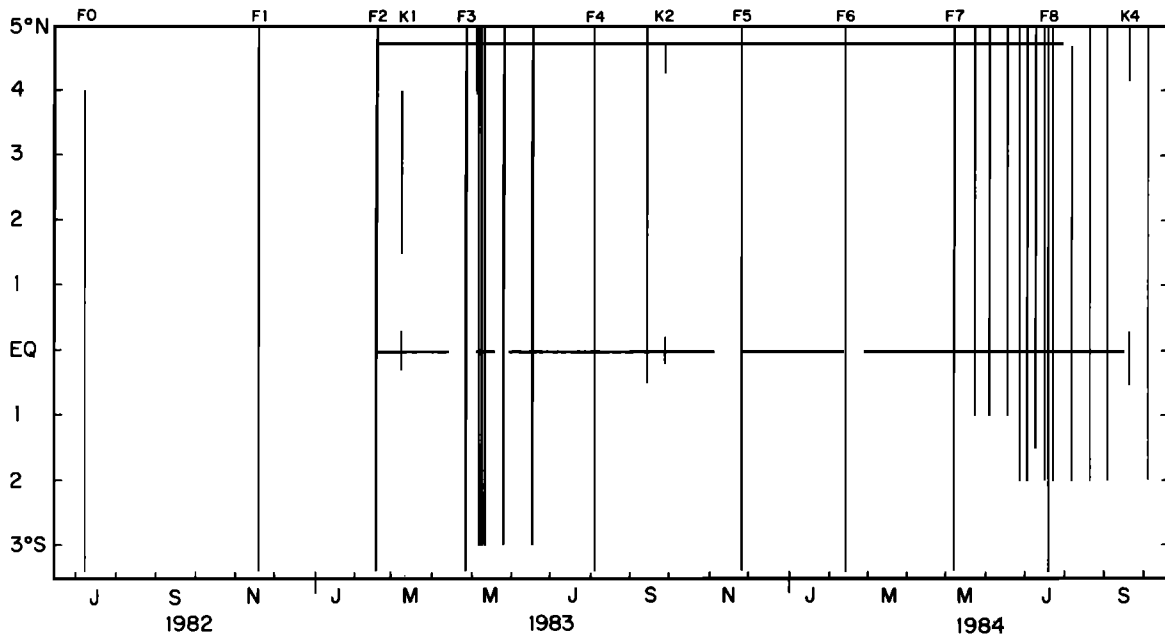
The CTD and AXBT sections were designed to pass near

Fig. 2.   The distribution of sections on 4°W. F0–F8 are the FOCAL CTD sections and K1–K4 are the SEQUAL XBT sections. Other vertical lines represent the SEQUAL AXBT sections. Data recovered from the FOCAL equatorial and coastal mooring are indicated by the heavy horizontal line.
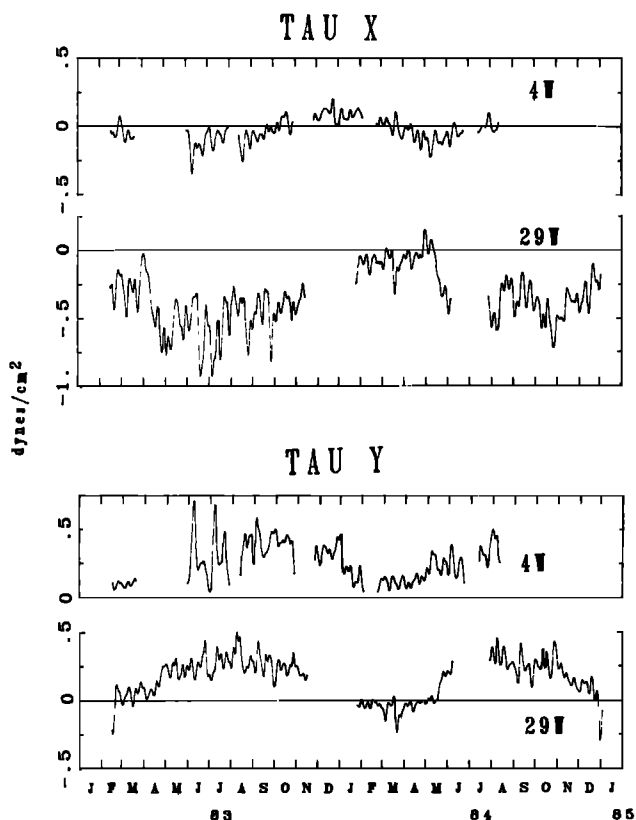
TAU X

TAU Y

Fig. 3. Low-passed (with 10-day cutoff) wind stress on the equator at 1°N, 29°W (courtesy S. L. Garzoli and E. J. Katz, 1984) and 0°, 4°W. Positive values are for eastward and northward stress.

the equatorial and coastal moorings, which provide even greater temporal resolution. The deployment of these moorings is shown by the heavy horizontal lines in Figure 2. The data derived from individual thermistors on the moorings have some additional gaps.

3. DESCRIPTION

Before examining the thermal data it is instructive to look at the wind data shown in Figure 3. The most striking feature is the sudden intensification of the zonal wind stress τx recorded at 29°W (positive is eastward) that coincides with a change in the sign of the meridional component (positive is northward). The date of this event (when τx becomes greater than 0.2 dyn/cm) is given by Katz et al. [1986] as April 11, 1983, and May 21, 1984. Thus the wind intensification in 1983 is 40 days or approximately 6 weeks earlier than in 1984 and about 2 months earlier than the climatological mean [Garzoli and Katz, 1984].

An apparent consequence of this time shift is shown in the sequence of GOSSTCOMP SST maps shown in Figure 4. Cooling at the equator in the western Gulf of Guinea occurs 4–5 weeks earlier in 1983. Otherwise, the patterns are very similar except for the absence of coastal upwelling along the eastern boundary in 1984. On the equator, cool water is first observed near 15°W. Subsequent upwelling along the eastern boundary and westward advection by the SEC produces the characteristic tongue of cold water seen in monthly mean SST map [e.g., Hastenrath and Lamb, 1977]. The cold SST derived from the coastal upwelling on the northern boundary is not resolved in the GOSSTCOMP maps.

The upwelling events associated with the cold SST are well resolved by the temperature sections along 4°W. The depth of
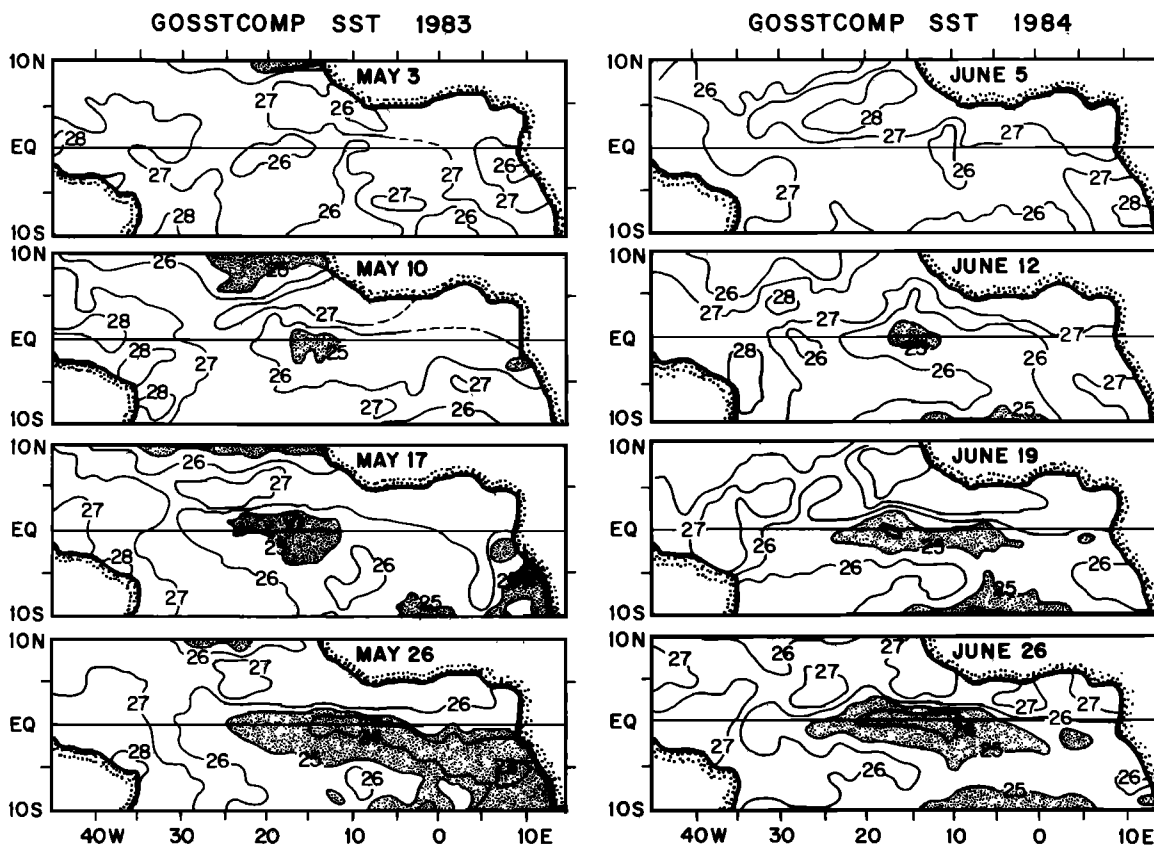
GOSSTCOMP SST 1983   GOSSTCOMP SST 1984

Fig. 4. Weekly GOSSTCOMP SST maps during the initial upwelling in 1983 and 1984. Dashed line indicates uncertainty due to cloud cover.

ISOTHERM DEPTH 4°W, 0.5°S–0.5°N
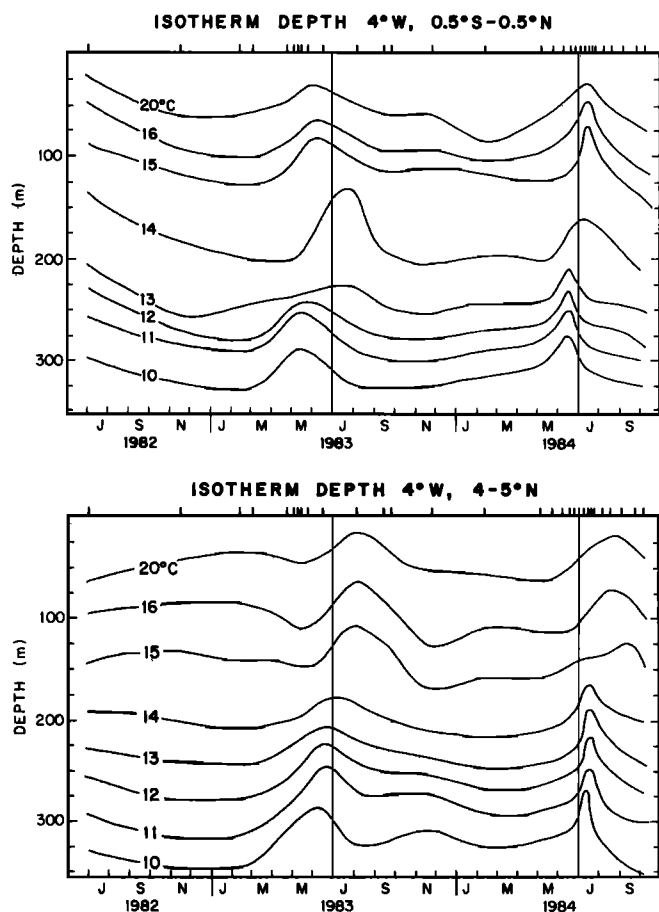

ISOTHERM DEPTH 4°W, 4–5°N

Fig. 5. Isotherm depth hand contoured from data along 4°W for the equator (top) and the coast (bottom). Vertical lines are shown for a time preference. Temporal distribution of data is given by tick marks at the top.

selected isotherms at the equator and the coast derived from these sections is shown in Figure 5. At all depths, except in the thermostad (125–200 m) where the weak vertical temperature gradients increase the variance, the vertical displacement of the isotherm associated with the seasonal upwelling is distinct. The signal is sharp, especially in 1984, and not well fitted by an annual harmonic. In all instances the phase at depth leads the surface and the equator leads the coast. A continuous vertical phase shift is not evident. Instead, especially at the equator in 1984, within the layers both above and below the thermostad the amplitude and phase of the upwelling signal appear to be independent of depth.

From these curves of isotherm depths it is difficult to pick an unambiguous definition of the timing of the upwelling event. Choices might include the time of the initial rise, the maximum vertical displacement velocity, the midpoint of the vertical displacement, or the peak. The coastal record in 1984 illustrates how each definition could lead to a different interpretation. For instance, the initial rise is earliest for the 20°C isotherm, the midpoint and maximum vertical velocity are nearly simultaneous throughout the water column, but the peak is earlier at depth. At the coast there is such a qualitative difference between the shape of these curves above and below the thermostad that it is doubtful that we are seeing a single event acting throughout the water column.

To illustrate the data from which the curves in Figure 5 are drawn and to investigate further these phase relationships, the depths of the 20°C, 11°C, and 12°C isotherms are shown in

Figure 6. The 20°C isotherm is chosen because it lies within the main thermocline and remains below the surface mixed layer. The 11°C and 12°C isotherms are within the deeper thermocline below the thermostad and are representative of the displacements observed there. In Figure 6, data for 1983 and 1984 are superimposed. Shown are the data points from which least squares cubic spline curves are calculated. For the 11°C and 12°C isotherms these data are the SEQUAL/FOCAL sections used in Figure 5, and each point in Figure 6 represents an average of three to six profiles. For the 20°C isotherm there are additional data. At the coast the depth of the 20°C isotherm at the shelf break (at the 100-m isobath) is derived from semiweekly coastal transects. At the equator and coast, additional data are provided by the moored thermistors.

A comparison of the equatorial mooring and section data (shown in Figure 7) is instructive, since time series data from the mooring were intended to provide temporal resolution unavailable from the CTD and AXBT sections. In Figure 7 the individual CTD and AXBT data points are shown, along with smooth curves hand drawn to fit a portion of these data. The fluctuating curves are derived from linear interpolation of filtered thermistor data with two exceptions. From mid-April to mid-May 1983 and mid-March to mid-May 1984 there are gaps in the record at 60 m depth so the interpolation is over a larger interval. Because of the position of the thermocline in February–March and July 1984, linear interpolation produced errors in the isotherm depth greater than 10 m. For these intervals, CTD and AXBT profiles are used to adjust the interpolated values.

It is somewhat surprising to see more fluctuation in the time series data. One would expect the CTD and AXBT measurements to be aliased by high-frequency fluctuations, while the mooring data are time averaged. However, the data points shown are an average of three to six profiles spanning 1° latitude and 2–10 hours time and have an average standard error of 3 m. The mooring data are measurements from a single point that are low-passed with a 10-day cutoff. Much of the fluctuation observed in the mooring data during May and June is due to meridional excursions of a thermal front. Nevertheless, the mooring data are useful in defining the minimum isotherm depth and filling in gaps, especially during early 1984. Otherwise, the CTD-AXBT data are adequate to resolve the upwelling event.

In Figures 6a and 6c we compare the thermocline (20°C) displacement associated with the equatorial and coastal upwelling in 1983 and 1984. For reference the climatic mean thermocline depth calculated from all data prior to 1980 is shown, as is the date of the trade wind intensification recorded at 29°W. In both years the minimum thermocline depth is the same and comparable to the climatic mean. In contrast, during the upwelling, the SST at the equator is close to the climatic mean in 1983 but approximately 1½°C warmer in 1984. The timing of the upwelling in 1984 is the same as the climatic mean at the coast and 1½ weeks early at the equator. In 1983 the upwelling is early by approximately 8 weeks at the equator and 2½ weeks at the coast.

During February 1984 the thermocline at the equator is approximately 30 m deeper than the climatic mean. This is about 3 standard deviations below the climatic mean depth, and thus it represents an anomalous condition. The meridional structure of this anomalous condition (see Figure 8) is roughly symmetric about the equator and extends to 110 m depth with a maximum at 90 m. At the coast (Figure 6) the thermocline is also depressed but by barely 1 standard devi-
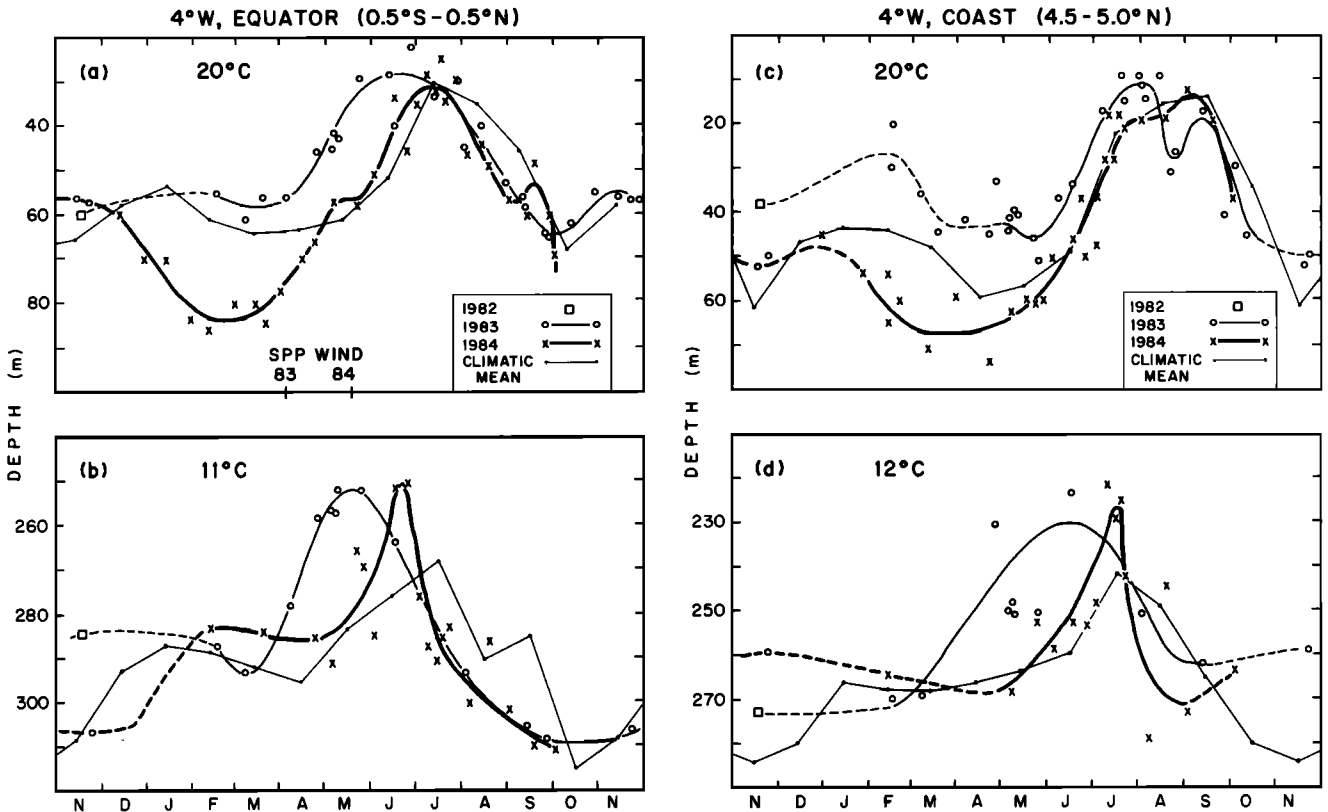
Fig. 6. Isotherm depth at the equator and coast associated with the main thermocline (20°C) and below the thermostad (11°C and 12°C). Straight-line segments are the climatic monthly mean. Solid lines are cubic spline least squares fits to the data points, which are averaged from three to six profiles. Dashed lines are hand-drawn fits to the remaining data.

ation below the climatic mean. FOCAL hydrographic sections along the equator (C. Colin et al., unpublished manuscript, 1986) show that this thermocline depth anomaly is greatest in the Gulf of Guinea and extends west to 20°W and that during this time the thermocline depth is nearly constant across the ocean basin west of 4°W. Mooring time series data (Figure 7) show that the anomalous deepening began December 1983, reached its maximum during February, and concluded late in April. The depression of the thermocline at the coast had a similar time dependence but did not represent such a statistically significant departure from the climatic mean.

With this in mind we now reexamine Figure 6. In 1984 the

thermocline at both the equator and the coast begins to shoal early in March. However, what appears to be a continuous process from March to July can be thought of as first a relaxation from an anomalous state followed by the seasonal upwelling beginning in May. It is the latter event which will result in cool SSTs. The amplitude of the isotherm displacement associated with each of these events is comparable as is
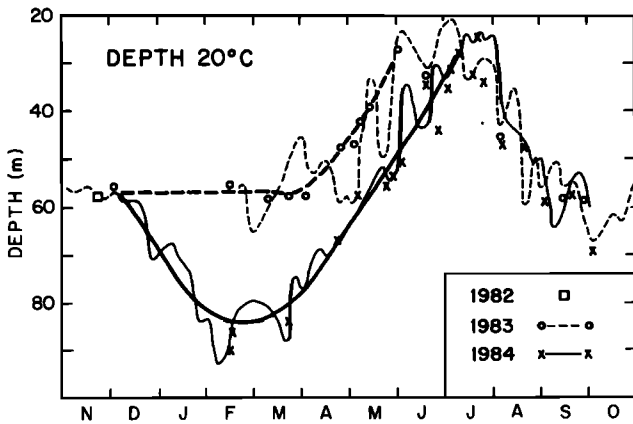

Fig. 7. Depth of 20°C, a comparison of hand-drawn (heavy solid) fit to CTD and AXBT data with the continuous interpolated depth from the FOCAL mooring data.
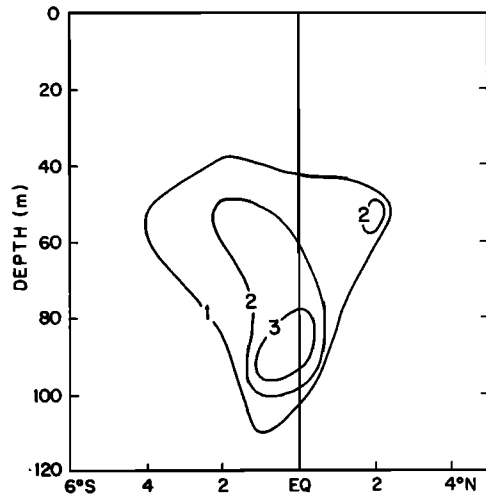

Fig. 8. Deviation of isotherm depths observed during the FOCAL 6 cruise in February 1984 below the climatic mean for months February–April in units of standard deviation from the climatic mean.
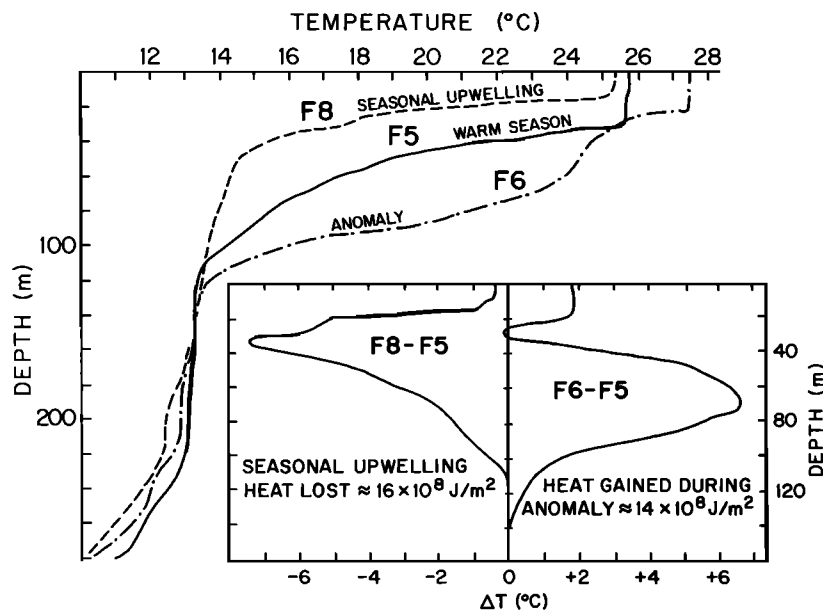
Fig. 9. Temperature profiles at 4°W, 0°N from FOCAL CTD data representing the normal "warm season" (F5, November 1984), the seasonal upwelling (F8, July 1984), and the anomaly (F6, February 1984). Also shown are profiles of the temperature change and integrated heat change between these states.

the change in the water column heat content. This is illustrated in Figure 9, where temperature profiles representative of the three states are shown. The heat gained during the anomaly is primarily due to the thermocline displacement with only a small contribution due to warming of the surface mixed layer.

Excluding the anomaly, the vertical displacements of the thermocline associated with the equatorial upwelling have the same amplitude in 1983 and 1984, with 1983 leading by approximately 6 weeks, which is the same as the lead in the time of the trade wind intensification to the west at 29°W. At the coast the upwelling amplitudes are also similar, but now 1983 leads 1984 by only $2\frac{1}{2}$ weeks. Beneath the thermostad there are less data, and the average standard error of the mean is 5 m, so the curve fit is less precise. But here also, isotherm displacements have approximately the same amplitude in 1983 and 1984, with 1983 earlier by more than 6 weeks at both the equator and the coast. Thus with the exception of the near-surface coastal upwelling, the timing of the upwelling events in the Gulf of Guinea appear to correspond approximately to the sudden intensification of the trade winds to the west. These phase relationships will be considered in more detail in section 4.

The meridional structure of the thermal field along 4°W for the two consecutive years is shown in the latitude versus time plots of the SST and depth of 20°C and 11°C isotherms in Figure 10. The seasonal cycle is evident in each of the fields, but there are notable differences. It is especially interesting to compare the SST and thermocline (20°C) depth. For instance, the anomaly during February 1984 which is so evident in the thermocline depth is not present at the surface or below the thermostad. Since the thermocline deepened during the warm season, the SST cannot become significantly warmer. During the annual upwelling the SST at the equator has a sharp meridional gradient, while the underlying thermocline topography, especially in 1984, is more symmetric about the equator. The thermocline shoaled to the same depth both years at the equator, but the SST was 1°–2°C warmer in 1984. At the onset of the upwelling, SST cooling is concurrent with thermocline shoaling, but then the SST remains cold long after the thermocline has returned to its original depth.

At the coast a different pattern is observed. During the upwelling the thermocline shoals for a longer period, and there is a better correlation between SST and thermocline depth. In both years the minimum SST and thermocline depth were the same magnitude. Cooler surface water associated with the coastal upwelling extends equatorward to approximately $3\frac{1}{2}$°N, whereas shoaling of the thermocline underneath extends farther south. There is some indication of the semiannual upwelling (i.e., the weak upwelling in December–January) in the thermocline data but only for 1983. Since few sections were taken during this time, it is not possible to resolve its timing or structure.

The thermal topography beneath the thermostad represented by the depth of the 11°C isotherm is similar to that of the thermocline, with important differences. The anomalous deepening in January–February 1984 is absent. The shoaling associated with the main upwelling at the equator and the coast has approximately the same duration. The upwelling is symmetric about the equator and more tightly bound to the coast, extending equatorward only to 4°N in 1983 and 3°N in 1984.

At the equator, isotherm displacements associated with the seasonal upwelling are observed throughout the water column. The vertical profile of this displacement field h is shown in Figure 11a. The displacement is calculated by taking the difference between the isotherm depth averaged over the preceding months, January–March (neglecting the 1984 thermocline anomaly), and the subsequent peak in June or July and assigning this value to the depth of the midpoint. For both 1983 and 1984, h is 30–40 m in the thermocline, increases to a maximum in the thermostad, decreases to a minimum of 20 m at 230 m, then increases again to 35 m at 280 m depth. The profile of h derived from the climatic data shows the same structure.

To obtain an estimate of the potential energy change associated with these displacements, we calculate h^2N^2, where N is the average Brunt-Väisälä frequency derived from the nine FOCAL sections. The profile of h^2N^2 (Figure 11b) has a maximum in the thermocline, a minimum at 225 m, and a relative maximum at 280 m depth. Values of N^2 range from 5.5 × 10^{-4} s^{-2} in the thermocline to a minimum of 0.2 × 10^{-4} s^{-2}

SST (°C) ALONG 4°W
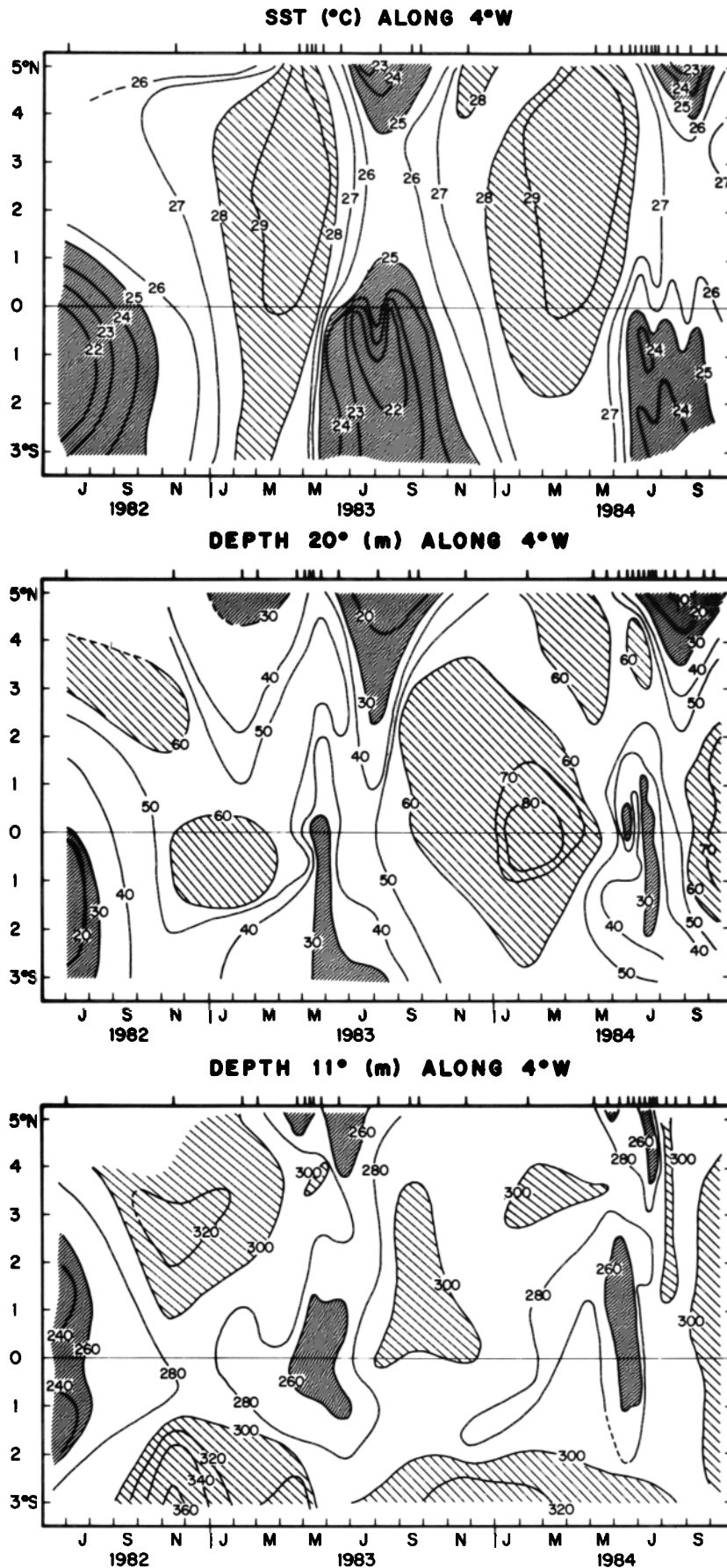
DEPTH 20° (m) ALONG 4°W

DEPTH 11° (m) ALONG 4°W

Fig. 10. Latitude versus time sections of SST and the topography of the thermocline depth (20°C) and subthermostad thermocline (11°C) hand contoured from data averaged over 1/2° latitude. Data distribution given by the tick marks at the top. Dashed line indicates extreme uncertainty due to gaps in data.
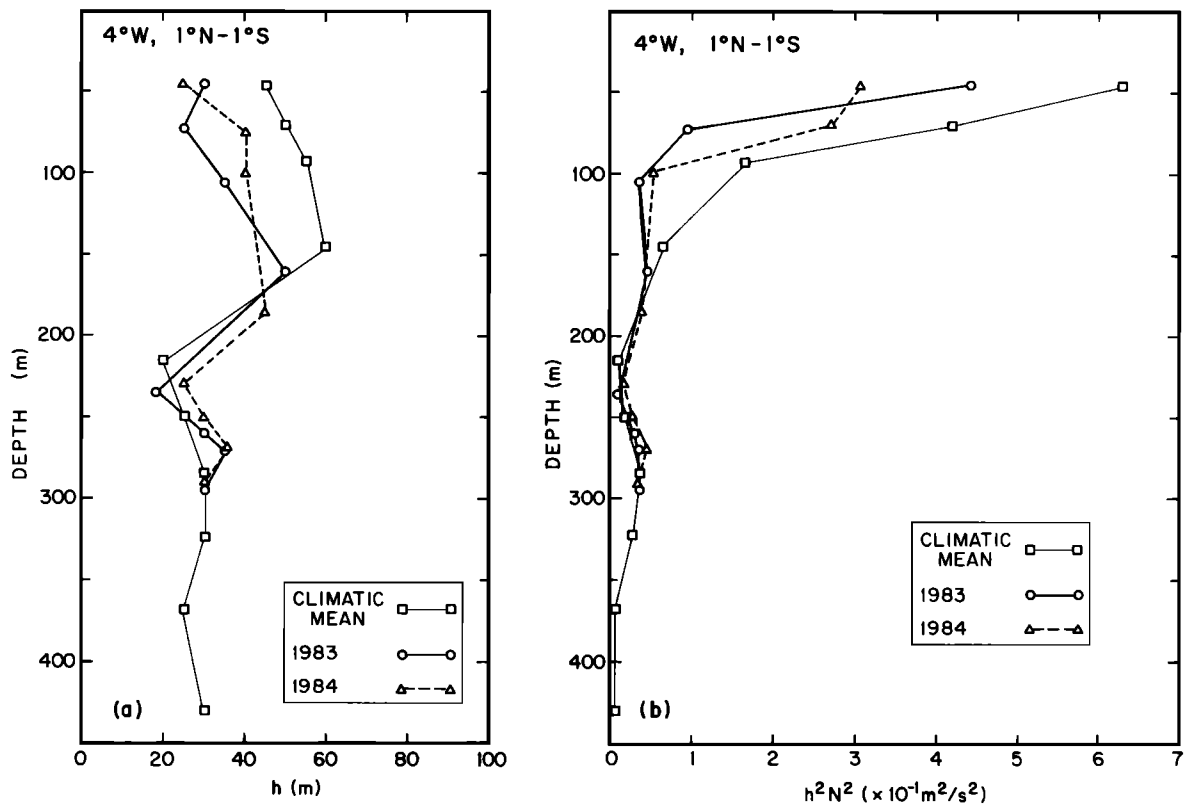
Fig. 11. Profiles of (a) isotherm displacement h (see definition in text) and (b) potential energy h^2N^2 associated with these displacements for 1983, 1984, and the climatic mean data.

in the thermostad between 125 and 200 m and then increase to a broad relative maximum of 0.4×10^{-4} s^{-2} centered at 290 m depth. Thus both h^2 and N^2 contribute to the relative minimum and maximum of h^2N^2 observed below the thermostad. The energy associated with the isotherm displacement at this depth is approximately an order of magnitude less than that of the thermocline displacements.

The meridional structure of h^2N^2 for 1983 and 1984 averaged together is shown in Figure 12. The contouring is derived from calculations averaged over 1° latitude centered at the dots. Largest values occur in the thermocline near the equator and the coast. The relative minimum with a subsequent maximum below extends from the equator to the coast. Separating the equatorial and coastal regimes is a relative minimum near 2°–3°N throughout the water column.

The question of the symmetry of this displacement field will be raised in section 4 when we identify the winds responsible for these isotherm displacements. The inherent noise in the data and the fact that few sections extend south of 2°S (see Figure 2) make a precise interpretation difficult. Although the structure of h^2N^2 for 1983 and 1984 is qualitatively similar, there are differences. In 1983 the displacement field both in the thermocline and at depth is symmetric about the equator, whereas in 1984 it is maximum at 1°S. South of 2°S the displacement diminishes at both levels, although the data there become sparse and noisy. The structure shown in Figure 12 suggests that the seasonal upwelling displacement field is more symmetric about the equator at 280 m than in the thermocline at 50 m depth.

4. ANALYSIS

The combined SEQUAL/FOCAL field program was successful in resolving the main seasonal upwelling for two con-secutive years. This signal was particularly robust within the thermocline and was still distinct, though noisier, at depth. The data show details of the temporal and spatial structure of the upwelling that are lost in the averaged climatic mean. The upwelling is a periodic but not sinusoidal event observed throughout the water column to 300 m depth. Interannual variability consists of differences in the timing but not the structure of the upwelling. Interpretation of the 1984 upwelling event is complicated by the fact that the thermocline was anomalously deep during the preceding January to March. The continuous shoaling of the thermocline from March to July appears to be a relaxation of this anomalous condition, followed by a normal seasonal upwelling.

Wind Forcing

The primary objective of this study is to distinguish the influence of local and far-field wind forcing on the thermal structure in the Gulf of Guinea. Wind data recorded at 4°W and 29°W (Figure 3) will be used to represent the local and far-field forcing since they are the only data that are reasonably continuous and complete. The wind intensification appears to be more abrupt at 29°W. This is associated with the local passage of the intertropical convergence zone (ITCZ). In the Gulf of Guinea, since the ITCZ remains north of the equator throughout the year, more gradual changes in wind speed are expected.

In both years, at 29°W, intensification of τx, the zonal stress, occurred over a 1-month interval. This intensification will be used as the primary time marker associated with the seasonal upwelling since there is no other event of comparable magnitude or duration in the wind data. Although subsequent wind fluctuations at 29°W have a magnitude comparable to the initial intensification event, the monthly mean during this

period is roughly constant. The predominant pattern in τx is a periodic step function rather than an annual harmonic. In contrast, the variation in τy and τx at 4°W and τy at 29°W is predominantly an annual harmonic. At 4°W there is a gap in the record during the intensification period in 1983. In 1984, however, τx increased (became more negative) over a 3-month interval beginning in February and was decreasing during May when τx and 29°W were increasing. Clearly, the intensification of τx recorded at 29°W and 4°W is not always simultaneous.

In addition to the annual upwelling the anomalously deep thermocline observed during December 1983 to April 1984 requires explanation. We look for an anomalous wind condition during that period. At 29°W, during January–March 1984, τx is nearly zero, significantly less than during the previous year. At 4°W, τx is positive from October 1983 to March 1984, and this is a departure from the climatic mean [*Hellerman and Rosenstein*, 1983]. Both of these factors would contribute to a deepening of the thermocline in the Gulf of Guinea. Associated with these anomalous winds is an extreme southern shift of the ITCZ (Y. Tourre, personal communication, 1986). At 4°W, τy is a minimum during January–March 1984 but does not appear to be any smaller than the previous year.

Equatorial Upwelling

During the equatorial upwelling in the Gulf of Guinea the thermocline shoals by approximately 30 m over a 2-month interval. The most precise temporal definition of this event is the time that the thermocline rises to the midpoint of this displacement. In 1984, because of the anomalous conditions preceding the upwelling, the vertical displacement is nearly 60 m over a $4\frac{1}{2}$ month interval. Above 60 m depth the curves of thermocline depth versus time (Figure 6a) for the 2 years are

1983   1984

EQUATOR   COAST

Main
Thermocline   May 3 → June 24   June 12 → July 10
                        52   28

                  ↑ 17 ──┼── 65 ↑   ↑ 6 ──┼── 18 ↑

Deep   4   16
Thermocline   April 16 → April 20   June 6 → June 22

DAY LAG
1984 – 1983

40	16
51	63

Fig. 13. The date of the annual upwelling event and associated time lags (in days) at the surface and depth for 1983 and 1984. Also shown is the day lag between the event in 1983 and 1984.

nearly parallel and are separated by approximately 40 days. Since this is identical to the lag of the wind intensification between 1983 and 1984 recorded at 29°W (44 days), we suggest that this upwelling is forced by the intensification of the zonal wind to the west of the Gulf of Guinea. The shoaling of the thermocline from 85 to 60 m depth during March–May is the relaxation from the anomalous state, an event separate from the seasonal upwelling.

The other curves in Figure 6 are analyzed in the same way to define the timing of upwelling events in the main thermocline and at depth at the equator and the coast. The results and the associated vertical, lateral, and 1984–1983 phase lags are given in Figure 13. In all cases, 1983 leads 1984, depth leads the surface, and the equator leads the coast.

It is difficult to estimate the accuracy of these times used to define the upwelling event. The upwelling process could be intermittent, so that the time of the event is not uniquely defined. Then there are high-frequency fluctuations that introduce noise into the data. We estimate the accuracy of the derived upwelling time from the variations in the fitted curve when the cubic spline calculations are adjusted. Since there are more data in the upper 100 m, timing of the upwelling in the main thermocline is determined more precisely, probably to within 1 week. Below 100 m, data are sparser and noisier, so the event time there is probably determined only to within 2 weeks at best. The curve fit to 12°C in 1983 at the coast is by far the most uncertain.

Even with these restrictions we can make some useful assessment of the phase lags given in Figure 13. At the equator the phase lag between 1983 and 1984 of the upwelling both at the surface and at depth is consistent with the lag observed in the intensification of the zonal wind at 29°W. There is a vertical phase shift of approximately 2 weeks. This appears to be across the thermostad and not continuous throughout the water column.

The timing of the coastal upwelling is different. In the thermocline the 1983–1984 lag is only 16 days, which is significantly different from the lag at the equator or in the wind intensification. Therefore the phase lag between the equator and the coast is not constant (52 days in 1983 and 28 days in 1984) as would be expected if the coastal upwelling is simply
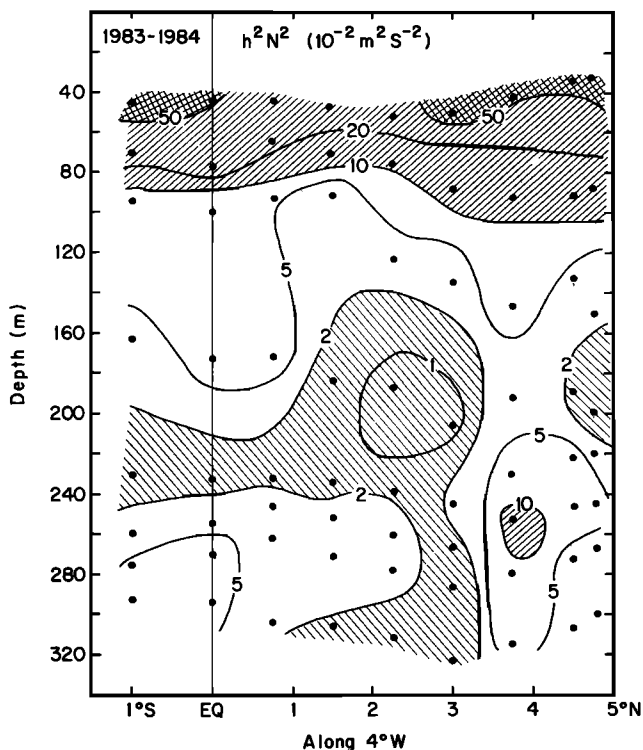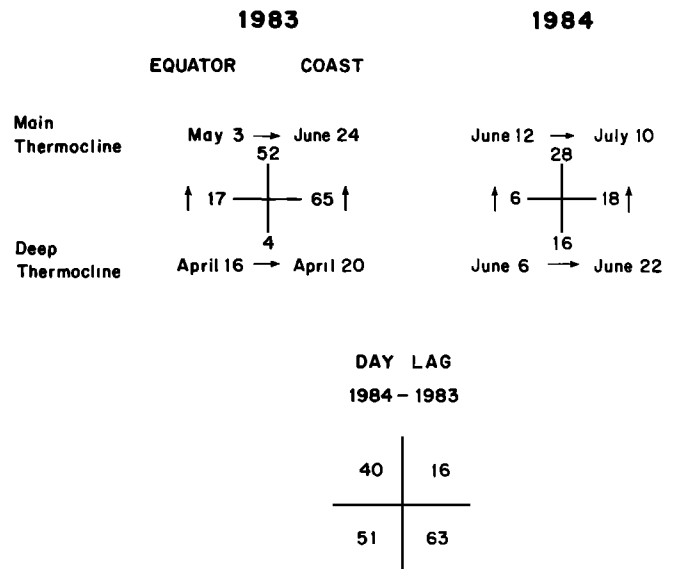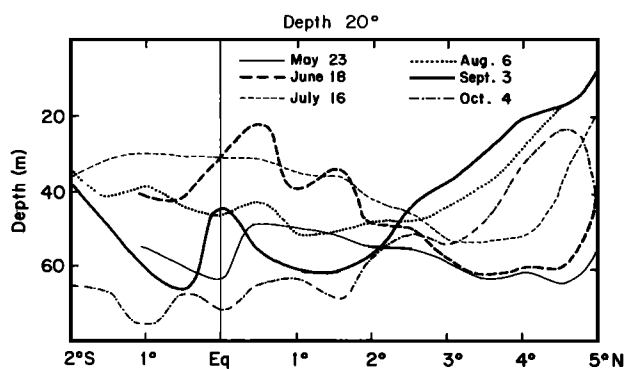
Fig. 12. A mean 1983–1984 meridional section of h^2N^2 hand contoured from calculations averaged over 1° latitude centered at each dot.

Fig. 14. Meridional sections of thermocline (20°C) depth, hand contoured from data averaged over 1/2° longitude for selected AXBT sections in 1984.

forced by a coastal trapped wave originating at the equator and propagating poleward around the eastern boundary.

At depth the timing of the coastal upwelling is more similar to the equator. The phase lag with the equator is 4 days in 1983 and 16 days in 1984. The 1983–1984 phase lag is 63 days. Considering the uncertainty in the data, especially in 1983 when the data were particularly noisy and sparse, these results suggest a possible correlation of the deep coastal upwelling with the equatorial upwelling and the intensification of τx in the west.

Coastal Upwelling

Of the four regimes illustrated in Figures 6 and 13 the upwelling of the thermocline at the coast is clearly the outlier. Not only does the upwelling there occur at approximately the same time each year, but also the isotherm shoaling persists 1 or 2 months longer than in the other regions. The coastal upwelling is associated with a sloping thermocline that often extends nearly to the equator. This is illustrated by the time sequence of the meridional structure of the thermocline depth shown in Figure 14. The shoaling of the 20°C isotherm, which is representative of the thermocline depth, is at first trapped close to the coast with a length scale less than 100 km but later extends equatorward with scales of 200–300 km. This is in contrast to the upwelling at depth (Figure 10) which remains trapped to within 100 km of the coast. Associated with the sloping coastal thermocline is the surface Guinea Current, a continuation of the North Equatorial Counter Current (NECC) as it enters the Gulf of Guinea. The seasonal variation of this current derived from direct measurement during the FOCAL cruises, geostrophic calculations from the AXBT sections, and the historical ship drift data (P. Richardson, personal communication, 1985) has the following characteristics. The speed increases during May and June from a value of 20–30 cm/s to a peak in July of approximately 70 cm/s. Subsequently, in August and September the high-velocity core of the Guinea Current veers offshore to lower latitudes.

We suggest, as originally proposed by Ingham [1970] and modeled by Philander [1979], that the coastal upwelling and the thermocline structure shown in Figure 14 are primarily the result of geostrophic adjustment to the Guinea Current. Because of the changing length scale and qualitative shape of the sloping thermocline (Figure 14), it is not likely that the Guinea Current is the result of geostrophic adjustment to a coastally trapped wave. Also, Ekman forcing by the local wind is not the dominant process since these length scales greatly exceed a local Rossby radius of deformation.

What drives the Guinea Current and determines its season-

al variation? It is interesting to note that the reversal of the NECC at 28°W, 6°N occurred in May for both 1983 and 1984 (P. L. Richardson and G. Reverdin, unpublished manuscript, 1986). Although the intensification of the NECC appears to be slightly later in 1984, there is definitely not the 6-week lag that is observed in the equator upwelling or in the intensification of τx in the west. The absence of a lag in the intensification of the Guinea Current between 1983 and 1984 could be the result of an inertial connection between the two currents or more likely the time dependence of the wind curl that drives both of these currents.

5. DISCUSSION

While the Gulf of Guinea thermal structure shown in Figure 10 resembles the climatic mean seasonal variation [*Houghton*, 1983], the 2-year SEQUAL/FOCAL data resolve rapid variation and interannual variability, which is averaged out in the climatic mean. The interannual variability between 1983 and 1984 has been useful in identifying links between the wind forcing and the ocean response. In particular, the nearly identical time lag between 1983 and 1984 in the intensification of τx at 29°W and the upwelling at 4°W suggests that this is the dominant forcing for the equatorial upwelling in the Gulf of Guinea. No other event in either the wind forcing or the ocean response is so distinctive and abrupt.

The role of local wind forcing in the Gulf of Guinea is more difficult to document since the wind stress is weaker and changes are less abrupt. In particular, τx at 4°W is approximately 1/4 of that at 29°W. During May and June 1984, τx at 4°W is decreasing so it can hardly be responsible for the upwelling at that time. However, τy at 4°W is increasing during this period and could contribute to forcing the local upwelling. The response to meridional wind forcing has two distinct characteristics. First, it is confined to the near surface, and second, it is asymmetric about the equator. The asymmetry will distinguish the response to local forcing from the symmetric forced Kelvin waves generated by τx to the west. *Philander* [1979] shows how a meridional wind stress will produce a broad upwelling south of the equator and downwelling to the north, creating a strong thermal front near the equator. Figure 10 does show a thermal front north of the equator, but the thermocline shoals at all latitudes. However, the thermocline upwelling appears to be greatest just south of the equator. FOCAL sections along 1°E and 6°E show that this asymmetry increases to the east (C. Colin et al., unpublished manuscript, 1986) where the meridional wind becomes more predominant. This is also seen in the SST (Figure 4). We conclude that the local meridional wind does influence the seasonal thermocline upwelling, but at 4°W this influence is only a perturbation to the dominant response forced by the zonal wind stress distributed to the west across the ocean basin.

The relatively precise timing of the wind intensification at 29°W and the upwelling at 4°W allows us to test simple ideas of free Kelvin wave radiation. Analysis of the phase lag of dynamic height perturbations from 35°W to 10°W (E. Katz, personal communication, 1986) yeilds a constant phase speed of 2.4 m/s, the speed of a first baroclinic Kelvin wave. Assuming this phase speed and simultaneous intensification of τx throughout the western equatorial Atlantic, we would project the forcing region to be 45°W, which is the region where τx is the largest. Ship of opportunity wind observations (J. Servain, personal communication, 1986) suggest that the intensification of τx is nearly simultaneous across the central and western equatorial Atlantic Ocean. However, time resolution of this wind field is limited to monthly averages.

Model calculation [*Philander and Pacanowski*, 1980] and the meridional scale length of the isotherm displacement field [*Houghton*, 1983] suggest that the seasonal upwelling in the equatorial Atlantic is associated with higher-mode Kelvin waves. The phase lag between the wind intensification at 29°W and the upwelling at 4°W is approximately 22 days for both 1983 and 1984, and this implies a phase speed of 1.3 m/s, close to a second baroclinic Kelvin wave. However, there is no evidence that the forcing region is localized near 29°W nor do the thermal displacements measured at 28°W [*Weisberg and Colin*, 1986] suggest free wave propagation.

The influence of the ocean boundaries and of various idealized distributions of zonal wind stress on the equatorial upwelling is illustrated by the linear two-layer reduced gravity model, with a phase speed of 1.6 m/s, of *Weisberg and Tang* [1985]. They have calculated the thermocline displacement forced by τx that intensifies linearly over a 1-month interval to a constant value with two different idealized zonal structures: (1) constant stress of 0.5 dyn/cm^2 from 5°W to 46°W, and (2) stress increasing linearly westward from zero at 5°W to 1 dyn/cm^2 at 46°W. Calculated thermocline displacements at 5°W are compared with the least squares fits to the observations at 4°W in Figure 15. The model winds intensify starting on April 6. The upwelling of the thermocline is due to a forced upwelling Kelvin wave generated by the integrated zonal stress to the west. The subsequent downwelling is the action of reflected Kelvin waves from the western boundary modified by reflected Rossby waves from the eastern boundary. The curves show that the two different wind distributions with the same integrated total stress change the thermocline displacement by 20%. The duration of the entire upwelling event, that is, the shoaling and subsequent deepening of the thermocline for winds that remain constant after intensification, is determined by the propagation time of reflection from the eastern and western boundaries. Model results derived from case 2 winds, which probably have the more realistic zonal structure and an amplitude chosen to fit the wind measurements at 29°W, best simulate the thermocline depth observed in 1983. These results are not changed significantly by more recent model calculations that include dissipation (R. H. Weisberg and T. Y. Tang, unpublished manuscript, 1986). In spite of high-frequency variations the mean τx at 29°W (Figure 3) remains approximately constant from May to October. Therefore the duration of the upwelling event observed in July and August 1983 is the result of ocean boundary reflections rather than a decrease in the wind stress.

Comparison of this model with 1984 observations raises additional questions. The upwelling amplitude is the same as in 1983, although τx appears to be approximately 25% weaker. The most striking difference is the duration of the upwelling event. The model calculation (not shown) by R. H. Weisberg and T. Y. Tang (unpublished manuscript, 1986) obtains a 1984 upwelling event that is shorter by approximately 1 week because of a slightly more rapid intensification of τx in 1984. However, we observe an upwelling event that is nearly 6 weeks shorter than the one in 1983 since it started 6 weeks later but concluded at the same time. Thus the earlier downwelling in 1984 that shortened the event is likely to be the result of a wind-forced downwelling rather than boundary reflections. The gap in the wind record (Figure 3) between June 15 and August 1 makes its interpretation ambiguous. There is a suggestion of a decline in τx during August, which, if sufficiently spatially coherent, could account for the earlier downwelling. Any further speculation as to the efficacy of this or other models requires the full SEQUAL wind field, still
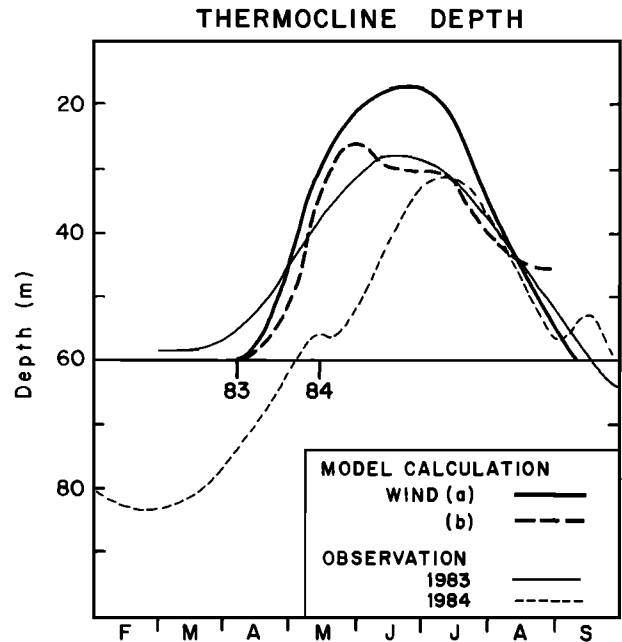
THERMOCLINE DEPTH

Fig. 15. Thermocline depth at 0°N, 4°W comparing model calculations of *Weisberg and Tang* [1985] with least squares fits to observations in 1983 and 1984. Vertical position of calculated curve adjusted to the mean thermocline depth prior to upwelling. Data of trade wind intensification at 29°W in 1983 and 1984 are also shown.

being processed, to resolve questions dependent on the details of the structure of the wind stress field.

The observation of isotherm displacements at the equator associated with the seasonal upwelling to 300 m depth beneath the thermostad is intriguing. These displacements lead the thermocline motion by approximately 2 weeks. Their symmetric structure about the equator and the coincidence of 1983 and 1984 time lag of this event and the trade wind intensification at 29°W suggest that they are forced by the zonal wind stress to the west of the Gulf of Guinea. Although the amplitudes of these displacements are comparable to those of the thermocline, the potential energy changes associated with them is approximately an order of magnitude smaller.

How does the energy associated with the seasonal upwelling penetrate to these depths at the equator? We note that the energy at depth is less than 10% of that at the surface, so most of the energy is trapped by and confined to the thermocline. However, it is curious that the energy associated with the isotherm displacements does not decrease monotonically with depth. Instead, there is a relative minimum near 230 m followed by a distinct relative maximum at 275 m, which coincides with the depth of a weak thermocline below the thermostad. A subthermocline maximum in the thermal displacement field in the central Pacific Ocean has been interpreted by *Lukas and Firing* [1985] as evidence of a beam of energy penetrating to depth. In this case the feature is centered off the equator, and it is identified as a westward propagating Rossby wave forced by the annual harmonic wind stress in the eastern Pacific Ocean. The feature we observe is centered at the equator so eastward propagating Kelvin waves forced to the west would be required. However, even if the linear theory by *McCreary* [1984] were applicable here, there are difficulties with a beam model. First, given the basin size and a realistic stratification, an annual harmonic ray path starting at the base of the mixed layer (~ 50 m) in the western equatorial Atlantic would barely penetrate to 100 m depth in the Gulf of Guinea. Second, to achieve the observed vertical scale of the deep

feature observed in the Gulf of Guinea requires wind forcing in the west with an unrealistically small horizontal scale. We note, however, that *Gent* [1985] has simulated the Pacific Ocean observations using a linear model and the distributed zonal wind stress over the entire Pacific Ocean.

Since at least several vertical modes are required to model a vertical phase shift, a simple two-layer model is not sufficient to describe all of our observations. The multilayer nonlinear model of *Philander and Pacanowski* [1984, 1986] does show seasonal isotherm displacements at depth; however, the amplitude is small, and the time dependence is unrealistic. Results of their linear calculations are even less realistic. This may be due to the fact that the model is forced by monthly mean winds of *Hellerman and Rosenstein* [1983], whose time dependence is dominated by the annual harmonic. We speculate that the impulsive nature of wind intensification observed in 1983 and 1984 may be an essential feature if the ocean response observed in 1983 and 1984, especially at depth, is to be modeled correctly.

We have shown that the character of the near-surface coastal upwelling is qualitatively different from that observed at the equator and have suggested that geostrophic adjustment to seasonal variations of the Guinea Current is a dominant factor. At depth, however, the coastal upwelling has an amplitude and duration that resemble more the upwelling at the equator than the thermocline above, especially in 1984. Unfortunately, the sparse and noisy data in 1983 preclude a reliable estimate of the 1983–1984 time lag in this upwelling event to compare with the equatorial wind intensification. In 1984 the coastal upwelling at depth lags the equator by 16 days, which implies an average phase speed of 2.6 m/s for propagation via the eastern boundary. Were it possible to discount the data from the FOCAL 4 cruise in April 1983, a similar phase shift could be deduced in the 1983 data (Figure 6*d*). The data, therefore, suggest but do not unambiguously define a fixed phase lag between the equatorial and deep coastal upwelling that would be required if the coastal event were forced by a wave propagating from the equator.

For a 5-month period early in 1984 the thermocline throughout the Gulf of Guinea was anomalously deep. Similar conditions have been observed in 1963 and 1968. Although the anomaly appears to be greatest in the Gulf of Guinea, it does extend over a larger region of the equatorial Atlantic. For instance, the zonal pressure gradient virtually vanished across much of the equatorial basin [*Hisard and Henin*, 1984; *Katz et al.*, 1986]. Both drifter [*Reverdin and McPhaden*, 1986] and profiler [*Hisard et al.*, 1986] current measurements detect a weakening and even a reversal of the south Equatorial Current early in 1984. This could be responsible for the large flux of heat into the Gulf of Guinea as the thermocline deepens and the warmer SST during the subsequent upwelling event.

Unusual conditions in the wind field (Figure 3) that could be associated with this anomaly are the very weak easterlies at 29°W during January to May and the westerlies at 4°W from October 1983 to March 1984. At 29°W, τx is definitely weaker in February 1984 compared to 1983. At 4°W, since there are only data during the months of August to February for one season, it is difficult to assess its interannual variability. However, the climatic mean τx [*Hellerman and Rosenstein*, 1983] for this period is zero so the observed τx of approximately 0.15 dyn/cm^2 is definitely more westerly than the mean.

The two noteworthy structural features of this thermal anomaly are its approximate symmetry at the equator (Figure 8) and its absence at depth below the thermostad (Figures 6

and 10). The first suggests that forcing by τx predominates. The second suggests that the forcing mechanism is different from that of the seasonal upwelling. The difference must be the structure of the wind stress field. From an inspection of the wind data in Figure 3 we suggest two factors. First, these wind field changes occur more slowly, 2–3 months, in contrast to the rapid intensification of the easterlies, and hence the response is confined to the near surface. Second, the wind in the Gulf of Guinea plays a more important role; that is, it is more of a local forcing problem. We note that model calculations by R. H. Weisberg and T. Y. Tang (unpublished manuscript, 1986) do generate deepening of the thermocline at 4°W from February to April 1984 in response to the decrease in τx to the west during the previous December but that the amplitude and duration are approximately 1/2 as large as our observations. Further speculation is not productive until models are forced with a basin-wide wind field that is realistic for 1983 and 1984. This wind field is presently being developed (V. Cardone, personal communication, 1986) using the European Center Medium Range Weather Forecast wind product, adjusted using ship wind observations.

6. CONCLUSIONS

The objective of this paper has been to describe the thermal structure observed in the Gulf of Guinea along 4°W during 1983 and 1984 with particular emphasis on those features that might resolve the long-standing question of local and far-field wind forcing of the seasonal upwelling. We have found a robust upwelling signal and distinct interannual variability in the wind forcing and ocean response. The upwelling amplitude for both years is the same, although the SST is warmer in 1984. The 1983–1984 time lag of the equatorial upwelling and the trade wind intensification is the same, while the time lag between the equatorial and coastal upwelling is different each year. The seasonal fluctuation in the thermal field is observed to depths as great as 300 m. In early 1984 the thermocline is anomalously deep. Although the anomaly is most pronounced in the Gulf of Guinea, it is associated with basin-wide features such as the absence of a zonal pressure gradient and a weakening and reversal of the south Equatorial Current. Some specific conclusions may be made at this stage of data analysis. These include the following: (1) the equatorial upwelling is forced primarily by τx distributed to the west of 4°W, (2) the asymmetry of this upwelling is due to the influence of the local meridional wind, (3) approximately 10% of this energy penetrates to depths below the thermostad, (4) the coastal thermocline upwelling is influenced primarily by the Guinea Current, (5) the deeper coastal upwelling may be forced from the equator via wave propagation on the eastern boundary, and (6) the 1984 anomaly is an event distinct from the seasonal upwelling and is probably more locally forced than is the seasonal upwelling.

All of these features appear to be sensitive to the spatial distribution and frequency content of the wind field. Previous model calculations by *Busalacchi and Picaut* [1983] and M. Cane (personal communication, 1986) indicate that the wind field throughout the entire equatorial Atlantic Ocean contributes to the forcing in the Gulf of Guinea. Further clarification of our observations will require calculations using a multilayer model forced by a realistic basin-wide wind field for 1983 and 1984.

REFERENCES

Adamec, D., and J. J. O'Brien, The seasonal upwelling in the Gulf of Guinea due to remote forcing, J. Phys. Oceanogr., 8, 1050–1060, 1978.

Bakun, A., Guinea current upwelling, Nature, 271, 147–150, 1978.

Berrit, G. R., Les eaux froides cotieres du Gabon à l'Angola sont-elles dues à un upwelling d'Ekman?, Cah. ORSTOM, Ser. Oceanogr., 14, 273–278, 1976.

Busalacchi, A. J., and J. Picaut, Seasonal variability from a model of the thermocline Atlantic Ocean, J. Phys. Oceanogr., 13, 1564–1588, 1983.

Colin, C., R. Chuchla, D. Corre, G. Hesloin, and M. Prive, Vents courants et temperatures observes du février 1983–octobre 1984 à 0°, 4°W Doc. Sci. ORSTOM, in press, 1986.

Garzoli, S. L., and E. J. Katz, Winds at St. Peter and St. Paul rocks during the first SEQUAL year, Geophys. Res. Lett., 11, 715–718, 1984.

Gent, P. R., The annual cycle in the central equatorial Pacific Ocean, J. Mar. Res., 43, 743–759, 1985.

Hastenrath, S., and P. J. Lamb, Climatic Atlas of the Tropical Atlantic and Eastern Pacific Ocean, 15 pp., 97 charts, University of Wisconsin Press, Madison, 1977.

Hellerman, S., and M. Rosenstein, Normal monthly stress over the world ocean with error estimates, J. Phys. Oceanogr., 13, 1093–1104, 1983.

Henin, C., P. Hisard, and B. Piton, Les eaux de l'Atlantique equatorial pendant l'opération FOCAL (juillet 1982–août 1984), Trav. Doc. ORSTOM, 196 pp., 1986.

Hisard, P., and C. Henin, Zonal pressure gradient, velocity and transport in the Atlantic Equatorial Undercurrent from FOCAL cruises (July 1982–February 1984), Geophys. Res. Lett., 11, 761–764, 1984.

Hisard, P., and J. Merle, Onset of summer surface cooling in the Gulf of Guinea during GATE, Deep Sea Res., GATE Suppl. 2–5, 26, 325–341, 1979.

Hisard, P., C. Henin, R. Houghton, B. Piton, and P. Rual, Oceanic conditions in the tropical Atlantic during 1983 and 1984, Nature, 322, 243–245, 1986.

Houghton, R. W., Circulation and hydrographic structure over the Ghana Continental Shelf during the 1974 upwelling, J. Phys. Oceanogr., 6, 910–924, 1976.

Houghton, R. W., Seasonal variations of the subsurface thermal structure in the Gulf of Guinea, J. Phys. Oceanogr., 13, 2070–2081, 1983.

Ingham, M. C., Coastal upwelling in the northeastern Gulf of Guinea, Bull. Mar. Sci., 20, 1–33, 1970.

Katz, E. J., P. Hisard, J. M. Verstraete, and S. L. Garzoli, Annual change of the zonal pressure gradient along the equator of the Atlantic Ocean in 1983/84, Nature, 322, 245–247, 1986.

Longhurst, A. R., The coastal oceanography of western Nigeria, Bull. Inst. Fr. Afr. Noire, Ser. A, 26, 337–401, 1964.

Lukas, R., and E. Firing, The annual Rossby wave in the central equatorial Pacific Ocean, J. Phys. Oceanogr., 15, 55–67, 1985.

McCreary, J. P., Equatorial beams, J. Mar. Res., 42, 395–430, 1984.

McCreary, J. P., J. Picaut, and D. W. Moore, Effect of annual remote forcing in the eastern tropical Atlantic, J. Mar. Res., 42, 45–81, 1984.

Mele, P. A., and R. W. Houghton, SEQUAL AXBT data report, 1983–1984, Rep. LDGO-85-3, 156 pp., Lamont-Doherty Geol. Obs. of Columbia Univ., Palisades, N.Y., 1985.

Mele, P. A., and E. J. Katz, Report of XBT data from four SEQUAL cruises, 1983–1984, Rep. LDGO-85-2, 160 pp., Lamont-Doherty Geol. Obs. of Columbia Univ., Palisades, N.Y., 1985.

Merle, J., Seasonal heat budget in the equatorial Atlantic Ocean, J. Phys. Oceanogr., 10, 464–467, 1980.

Moore, D., P. Hisard, J. McCreary, J. Merle, J. O'Brien, J. Picaut, J. M. Verstraete, and C. Wunsch, Equatorial adjustment in the eastern Atlantic, Geophys. Res. Lett., 5, 637–639, 1978.

Philander, S. G. H., Upwelling in the Gulf of Guinea, J. Mar. Res., 37, 23–33, 1979.

Philander, S. G. H., and R. C. Pacanowski, The generation of equatorial currents, J. Geophys. Res., 85, 1123–1136, 1980.

Philander, S. G. H., and R. C. Pacanowski, Simulation of the seasonal cycle in the tropical Atlantic Ocean, Geophys. Res. Lett., 11, 802–804, 1984.

Philander, S. G. H., and R. C. Pacanowski, Nonlinear effects in the seasonal cycle of the tropical Atlantic Ocean, Deep Sea Res., in press, 1986.

Picaut, J., Propagation of the seasonal upwelling in the eastern equatorial Atlantic, J. Phys. Oceanogr., 13, 18–37, 1983.

Reverdin, G., and M. J. McPhaden, Near-surface current and temperature variability observed in the equatorial Atlantic from drifting buoys, J. Geophys. Res., 91, 6569–6582, 1986.

Servain, J., J. Picaut, and J. Merle, Evidence of remote forcing in the equatorial Atlantic Ocean, J. Phys. Oceanogr., 12, 457–463, 1982.

Verstraete, J. M., Étude quantitative de l'upwelling sur le plateau continental Ivorien, Doc. 1, pp. 1–17, Sci. Cent. de Rech. pour Oceanogr., Abidjan, Ivory Coast, 1970.

Voituriez, B., The equatorial upwelling in the eastern Atlantic Ocean, Report of the Final Meeting of Scientific Committee on Oceanic Research, WG47, pp. 229–247, Nova Univ. Press, Fort Lauderdale, Fla., 1981.

Weisberg, R. H., and C. Colin, Upper ocean temperature and current variations along the equator in the Atlantic Ocean during 1983–1984. Nature, 322, 240–243, 1986.

Weisberg, R. H., and T. Y. Tang, On the response of the equatorial thermocline in the Atlantic Ocean to the seasonally varying trade winds, J. Geophys. Res., 90, 7117–7128, 1985.

C. Colin, ORSTOM, Department of Marine, Earth and Atmospheric Sciences, North Carolina State University, Raleigh, NC 27695.

R. W. Houghton, Lamont-Doherty Geological Observatory of Columbia University, Palisades, NY 10964.